Tribology and Materials
Vol. x, No. x, 202x, pp. xx-xx

ISSN 2812-9717
https://doi.org/10.46793/tribomat.202x.xxx

Correlation of microstructure and mechanical properties of the aluminium alloy 6061 reinforced with seashell particles

Riki Hendra PURBA *, Septia SAHARANI, James JULIAN , Fathin Muhammad MAHDHUDHU ,
Fitri WAHYUNI , Elvi ARMADANI

Universitas Pembangunan Nasional Veteran Jakarta, Jakarta, Indonesia
*Corresponding author: rikihendrapurba@upnvj.ac.id

Keywords

aluminium matrix
Anadara granosa
microstructure
renewable material
mechanical properties

History

Received: 29-11-2025
Revised: 16-06-2026
Accepted: 28-07-2026

Abstract

The increasing demand for renewable reinforcement materials has encouraged the exploration of abundant biomaterial waste as an alternative to conventional ceramic reinforcements in metal matrix composites. In this study, *Anadara granosa* shell powder (AGSP), an underutilised and widely available biogenic waste, was investigated as an eco-friendly reinforcement for aluminium alloy 6061 (Al6061). The samples were produced via sand casting using AGSP. There were three different AGSP sizes: 120, 180 and 200 µm added to the Al6061 alloy. Microstructural analysis, density measurements and tensile testing were conducted to assess the impact of AGSP additions of different sizes on the Al6061 alloy. The findings reveal that finer particles promote a more homogeneous distribution, enhanced interfacial bonding, reduced porosity and more efficient load transfer, resulting in improved tensile performance. Conversely, coarser particles exhibit less uniform dispersion and lower mechanical properties. Meanwhile, the density of Al6061 exhibited no significant variation, suggesting that the addition of AGSP reinforcement does not diminish the inherent lightweight advantage of the Al6061 alloy. Overall, the study demonstrates the strong potential of *Anadara granosa* shell waste as a renewable, low-cost and effective reinforcement for aluminium alloys, while highlighting the critical role of particle size selection in optimising composite quality.

1. Introduction

Aluminium alloy 6061, an Al-Mg-Si alloy, is one of the most extensively used commercial aluminium grades, particularly in metal matrix composite (MMC) applications. Aluminium-based MMCs have gained significant attention due to their ability to combine the lightweight characteristics of aluminium with enhanced mechanical performance derived from ceramic particulate reinforcements [1]. Various reinforcement materials, including SiC, Al_2O_3, B_4C, graphene and high-entropy alloy (HEA) particles, have been incorporated into aluminium matrices to tailor microstructure and improve strength, hardness and wear resistance [2-5]. However, previous reinforcement methods tend to be costly and raise concerns regarding environmental sustainability. In recent years, there has been growing interest in incorporating reinforcement sourced from biomaterial waste into MMCs, supporting sustainable materials development by utilising abundant biogenic waste.

Anadara granosa, commonly known as the blood cockle, is widely consumed as a food source, resulting in large quantities of shell waste that are often discarded and contribute to environmental pollution. Structurally, the shells comprise three functional layers: the periostracum as the protective outer coating, the prismatic layer composed of calcium carbonate crystals arranged in prism-like formations and the nacreous layer formed by stacked aragonite platelets. The synergy of these layers yields a naturally strong and durable bioceramic structure with microstructural features that make the material a promising candidate for composite reinforcement [6].

Chemically, *Anadara granosa* shells consist primarily of calcium carbonate, mainly in the form of calcite, aragonite and vaterite, with reported purities reaching up to 97.53 wt. % [5,7]. Previous studies on biomaterial-derived $CaCO_3$ reinforcements, including eggshells and mussel shells, have demonstrated improvements in hardness, tensile strength and yield strength when incorporated into aluminium-based matrices [8,9]. However, studies on AGSP as a reinforcement in aluminium-based MMCs remain limited, particularly regarding its mechanical and microstructural performance. Extensive studies on the development of AGSP and the use of various reinforcement types in aluminium alloy 6061 matrices have been reported and are summarised in Table 1.

Nevertheless, a critical review of the literature reveals that the use of *Anadara granosa* as a reinforcing particle in aluminium alloy 6061 remains largely unexplored and has not been comprehensively addressed. Furthermore, existing studies have predominantly focused on the influence of the reinforcement weight fraction, with limited attention to the effects of particle-size variation on mechanical response and microstructural evolution. Meanwhile, particle size is a critical factor influencing particle distribution, interfacial bonding, porosity levels, crack initiation behaviour and overall load transfer efficiency within MMCs. To address this gap, the present study investigates the influence of AGSP size (120, 180 and 200 µm) on the microstructure and mechanical behaviour of aluminium alloy 6061 (Al6061), contributing to the development of lightweight, high-strength aluminium-based composites for structural applications.

Table 1. Summary of related previous studies

Reference	Material	Summary
Sinurat et al. [6]	AGSP	CaO prepared from AGSP via calcination at 600−1000 °C and used as a precursor for hydroxyapatite synthesis
Nasir et al. [7]	AGSP	AGSP incorporated as a glass component in glass ionomer cement and characterised via FTIR
Al Fath et al. [10]	AGSP	AGSP converted into chitosan for biobattery application
Saraswati et al. [11]	AGSP	$CaCO_3$ from shell applied to dental pulp and NF-κB, TGF-β1 and VEGF-A expression analysed
Siswoyo et al. [12]	AGSP	Shell used as natural coagulant to reduce total suspended solids and turbidity in well water
Ruslan et al. [13]	AGSP	Shell waste used as partial fine aggregate replacement in mortar for sustainable construction
Veeresh Kumar et al. [2]	6061	6061-SiC and 7075-Al_2O_3 composites fabricated via liquid metallurgy with 2−6 wt. % reinforcement, evaluated for hardness, tensile and wear properties
Deng et al. [4]	6061	Aluminium matrix reinforced with TiB_2 and B_4C for improved mechanical properties
Gassour et al. [14]	6061	Tribological performance improved by reinforcing 6061 with green-synthesised silver nanoparticles
Muhammed Muneer et al. [15]	6061	6061 reinforced with AlNbTaZr-Al_2O_3 for better structural, mechanical and wear behaviour
Beldar and Kumavat [16]	6061	Mechanical properties of 6061-Ni and 6061-Cr composites investigated at 0−2.7 wt. % reinforcements variation
Bharathiraja and Anthony Xavior [17]	6061	The effect of graphene, B_4C and T6 heat treatment on the microstructural and mechanical properties of 6061 matrix composites
Ghadimyari and Akhlaghi [18]	6061	AlFeCuCrNi particles added in varying volume fractions to 6061 via powder metallurgy
Kandpal et al. [19]	6061	6061/Al_2O_3 composites fabricated by stir casting had refined grains and improved microhardness and tensile strength with increasing Al_2O_3 content

2. Materials and methods

2.1 Samples preparation

The chemical composition of Al6061, shown in Table 2, has been verified using the Vanta handheld X-ray fluorescence analyser and compared with a standard to ensure material suitability before the fabrication process.

Table 2. Chemical composition of Al6061, wt. %

Element	Present study	ASTM B209 [20]
Mg	1.09	0.8 – 1.2
Si	0.76	0.4 – 0.8
Fe	0.31	max. 0.7
Cu	0.17	0.15 – 0.40
Mn	0.23	max. 0.15
Cr	0.05	0.04 – 0.35
Zn	0.06	max. 0.25
Al	balance	balance

It has been previously reported that AGSP contains $CaCO_3$, with minor oxide components also identified, including Al_2O_3, Na_2O and SiO_2 [21]. These biomaterial components highlight the potential of AGSP as an environmentally friendly reinforcement material while helping reduce shell waste pollution. However, to obtain accurate data, X-ray diffraction (XRD) analysis of AGSP was performed using a Rigaku MiniFlex 600 X-ray diffractometer to identify the crystallographic phases prior to reinforcement. The analysis was conducted at a tube current of 15 mA and a tube voltage of 40 kV using a Cu tube.

The influence of mussel shell powder (MSP) reinforcement on the mechanical properties of 6061 alloy was investigated in a previous study [9], which revealed that a 15 wt. % MSP addition exhibited the highest hardness and tensile strength. Based on that study, approximately 15 wt. % of AGSP was added in the present study. Prior to the solidification process, the *Anadara granosa* shells were collected from seafood waste, washed with a Bayclin disinfectant solution and powdered detergent to remove contaminants and then dried in sunlight for two hours. The dried shells were ground with a mortar and pestle, then sieved into different particle-size fractions. The actual average particle sizes of the sieved fractions were measured using ImageJ software and found to be 120, 180 and 200 µm, respectively.

Composite samples were manufactured using the sand casting method, consisting of Al6061 reinforced with 15 wt. % AGSP. The procedure began by calculating the required amounts of Al6061 (2.7 g/cm^3) and AGSP (1.3 g/cm^3). Then, the Al6061 alloy was melted in a furnace at approximately 700 °C. After that, AGSP reinforcement was added to the melt and manually stirred for 30 minutes at approximately 700 °C to ensure the homogeneous distribution of AGSP in the molten Al6061. Then, the melt was poured into a bar-shaped sand mould with dimensions 400 × 250 × 10 mm. Finally, the melt was cooled at room temperature for approximately three hours.

2.2 Microstructure analysis

Microstructural characterisation is essential for understanding the internal phase distribution and the quality of particle–matrix interfaces. Characterisation was performed using an optical microscope and scanning electron microscope (SEM) with energy-dispersive X-ray spectroscopy (EDS).

The optical microscope was primarily used to examine the samples to evaluate the effectiveness of particle mixing and bonding. SEM provided high-resolution images to confirm the morphology of the reinforcement particles, detail the quality of the interface bonding between the matrix and the reinforcement and identify porosity, all of which significantly influence mechanical performance. Additionally, EDS was utilised to determine the chemical composition of the embedded reinforcement. In addition, ImageJ software, which supports SEM images, was used to calculate the size distribution of AGSP particles.

2.3 Physical and mechanical testing

Density measurements were performed using the mass-to-volume ratio method, where density equals mass divided by volume. The mass of each specimen was measured using a precision balance with an accuracy of ± 0.001 g, while the volume was determined by measuring cubic specimens with dimensions of 1 × 1 × 1 mm. Three replicate measurements were conducted for each sample to ensure accuracy and repeatability of the results. The average density value was calculated from these three measurements, and the standard deviation was used to assess the consistency of the data.

The tensile test was conducted in accordance with the ASTM E8/E8M standard. Samples were machined using CNC milling to standard tensile test dimensions. A VTS WAW-600E universal testing machine was used to determine the strength of materials until fracture occurred, with three repeated tests at 0.02 mm/s. The tensile sample geometry is shown in Figure 1.

Figure 1. Tensile test samples

3. Results and discussion

3.1 Microstructure

In general, the performance of alloys and composites is governed by their microstructures. Accordingly, detailed microstructural characterisation of the samples was carried out in the present study. The XRD analysis (Fig. 2) was performed to identify the crystalline phase of AGSP. The diffraction pattern reveals that AGSP is predominantly composed of aragonite ($CaCO_3$), as indicated by the characteristic peaks at 2θ values corresponding to the aragonite phase. This finding is consistent with previous studies on marine shell-based materials [21]. The presence of aragonite as the dominant phase is significant for reinforcement

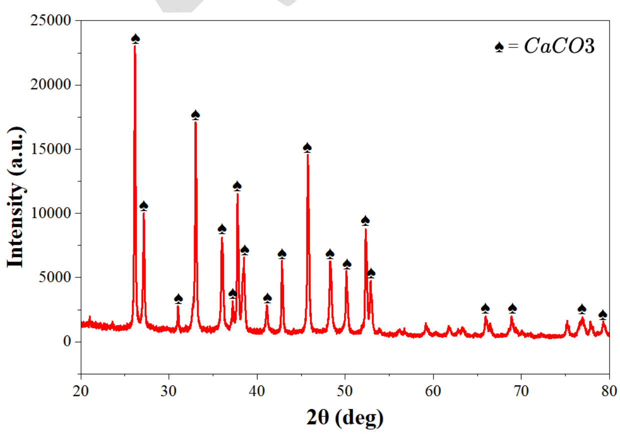

Figure 2. XRD pattern of AGSP

applications due to its distinct mechanical properties compared to other $CaCO_3$ polymorphs.

Figure 3 shows the microstructure of an unreinforced Al6061 alloy. The microstructure is shown in grey and white. Previous literature has identified the grey area as corresponding to the Mg_2Si phase and the white area to the Fe-rich insoluble phase [22]. Figure 4 displays the microstructure of composites produced with average AGSP particle sizes of 120, 180 and 200 µm. In the micrographs, the AGSP phase appears as bright areas, while the darker areas correspond to the Al6061 alloy. The same result has been reported in our previous study [23]. However, it was used to study the influence of AGSP size on the toughness and hardness of Al6061. The particle size distribution shows that finer particles enforce stricter selection, allowing only smaller particles to be incorporated into the matrix. Consequently, reducing particle size increases the specific surface area of the reinforcement, which enhances matrix-particle interaction and promotes better dispersion within the composite [24].

The elemental distribution was examined through EDS mapping as shown in Figure 5. Carbon (C-K) and calcium (Ca-K), indicated by cyan regions, confirm the AGSP particle locations within the Al6061 alloy. Aluminium (Al-K) mapping shows uniform matrix distribution, while oxygen (O-K) concentrates in AGSP regions, consistent with calcium carbonate composition. Magnesium (Mg-K) appears scattered in the matrix, associated with the Mg_2Si phase. Silicon (Si-K) shows minimal presence due to low concentration. The clear elemental demarcation between Ca-rich AGSP and Al-rich matrix confirms successful reinforcement incorporation and uniform particle dispersion.

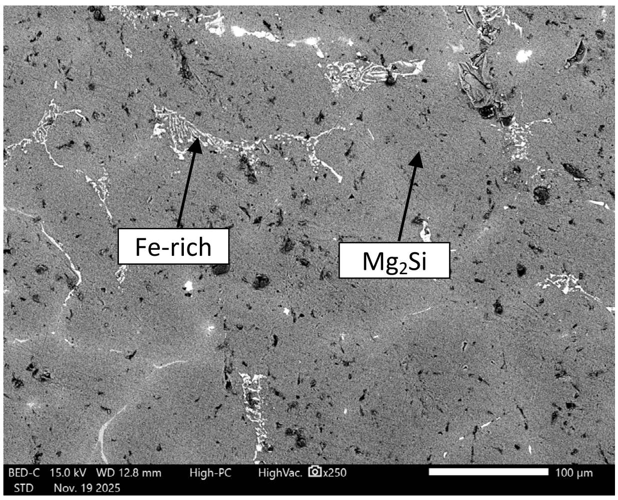

Figure 3. SEM morphology of Al6061 without reinforcement

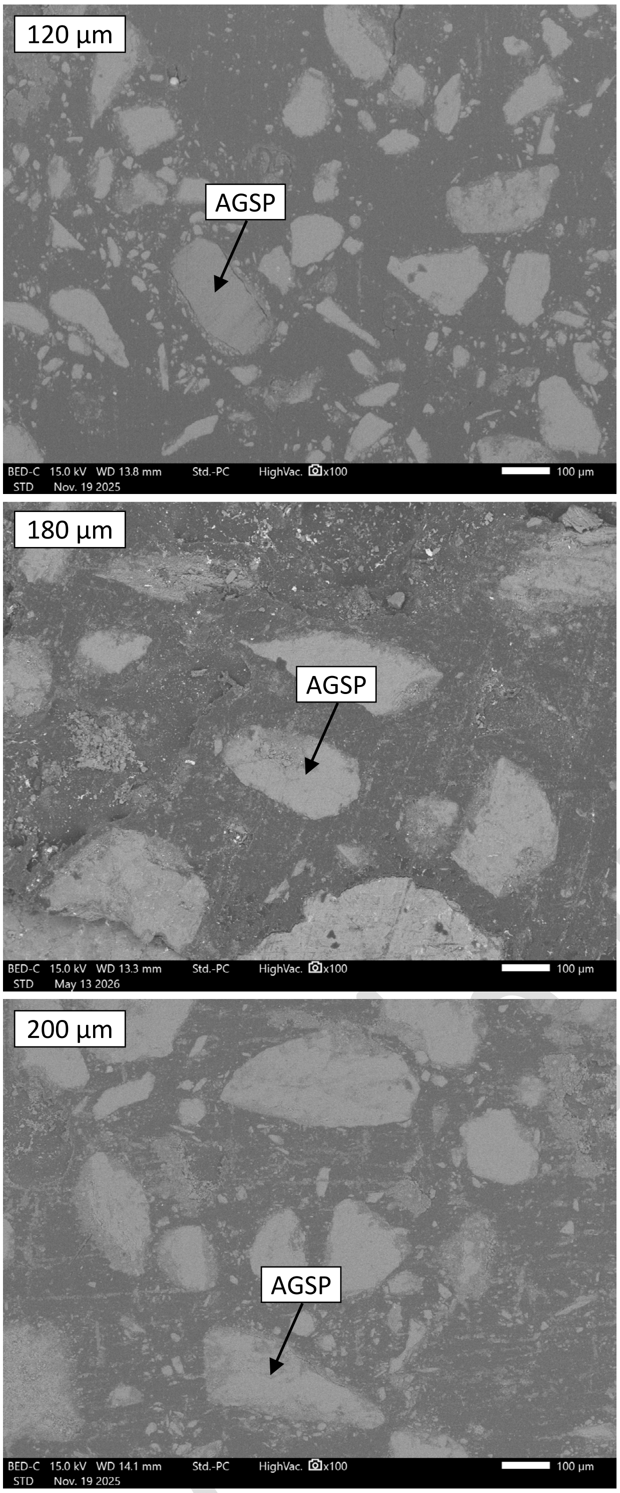

Figure 4. SEM morphologies of Al6061 reinforced with AGSP

The EDS analysis was utilised to obtain the chemical composition of AGSP, and the results are given in Figure 6. The AGSP composition (average size 180 µm) is provided in Table 3. The analysis results, as shown in Figure 6, indicate that the powder is dominated by calcium and oxygen, indicating that calcium oxide or calcium carbonate forms the main phase. EDS analysis revealed 19.92 wt. % carbon, 40.86 wt. % oxygen, 0.72 wt. % sodium, 0.17 wt. % aluminium, 0.24 wt. % silicon and 38.09 wt. % calcium. The Si peak is not visible in the EDS spectrum due to its very low concentration in the AGSP region, making it difficult to detect in the graphical representation, although it was quantified in the tabulated data. The presence of Ca, O and C as the dominant elements confirms that the AGSP is predominantly composed of $CaCO_3$, which is consistent with the reference composition reported in the literature [7]. Similar $CaCO_3$-rich compositions have been reported for waste oyster shells and other marine shell-based materials [24].

Table 3. Elemental composition of AGSP determined by EDS analysis of AGSP with particle size of 180 µm

Element	Line	wt. %	at. %
C	K	19.92 ± 0.22	31.84 ± 0.35
O	K	40.86 ± 0.70	49.03 ± 0.84
Na	K	0.72 ± 0.06	0.60 ± 0.05
Al	K	0.17 ± 0.02	0.12 ± 0.02
Si	K	0.24 ± 0.03	0.16 ± 0.02
Ca	K	38.09 ± 0.35	18.25 ± 0.17

3.2 Density

One of the key advantages of Al6061 alloy is its lightweight characteristic, making density a critical property to maintain in composite applications. The density measurements for unreinforced Al6061 alloy and AGSP-reinforced composites with different particle sizes are presented in Figure 7. The results show that the matrix (Al6061 alloy) exhibits an average density of 2.80 g/cm^3, which is in good agreement with the standard density of aluminium at 2.7 g/cm^3 [25]. The addition of 15 wt. % AGSP with varying particle sizes resulted in slight variations in composite density. The composite reinforced with 200 µm AGSP particles showed an average density of 2.56 g/cm^3, while those with 180 and 120 µm particles exhibited densities of 2.31 and 2.43 g/cm^3, respectively. These values are comparable to those reported in previous studies on 6061 alloy-based composites reinforced with lightweight particles. For instance, 6061-graphite composites with 6 to 12 wt. % reinforcement showed densities ranging from 2.48 to 2.59 g/cm^3 [26], which aligns with the trend noticed in the present study, where the incorporation of low-density reinforcement materials leads to a reduction in overall composite density.

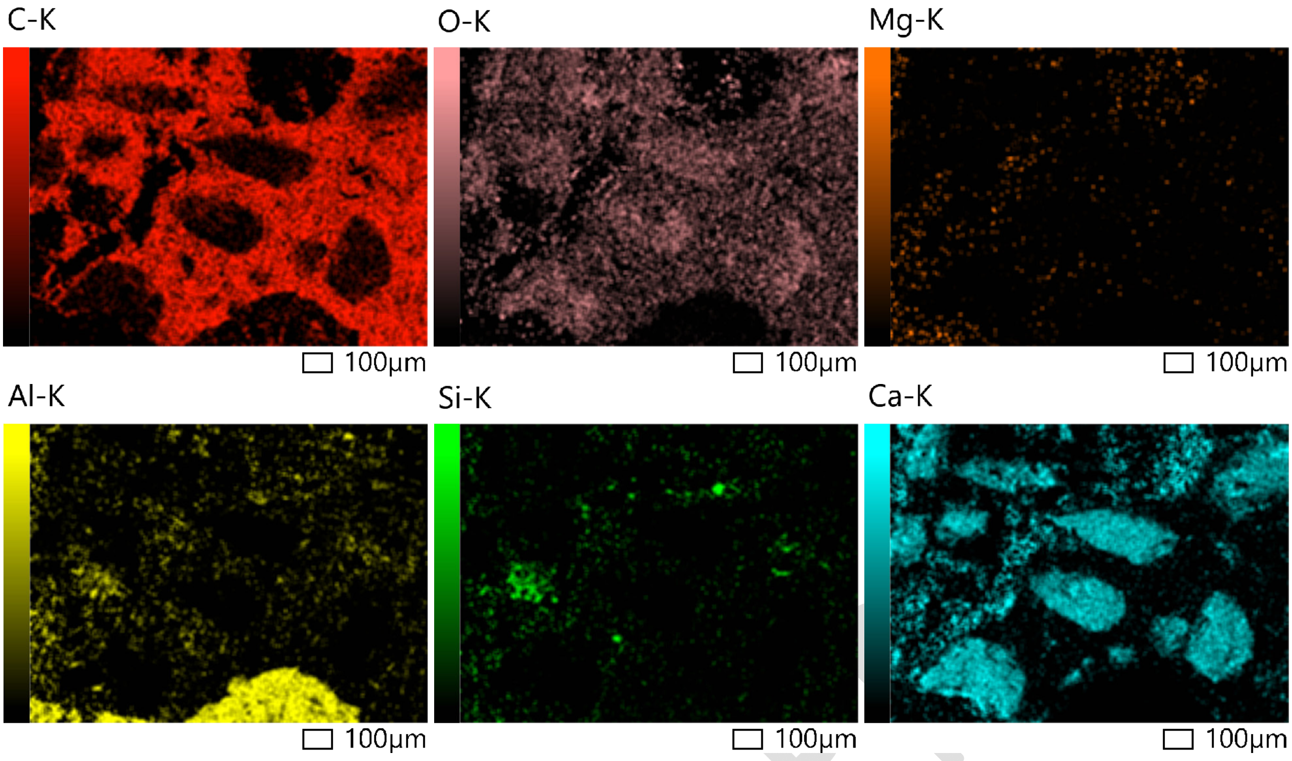

Figure 5. EDS elemental mapping of Al6061 reinforced with AGSP particle sizes of 180 μm as a representative sample

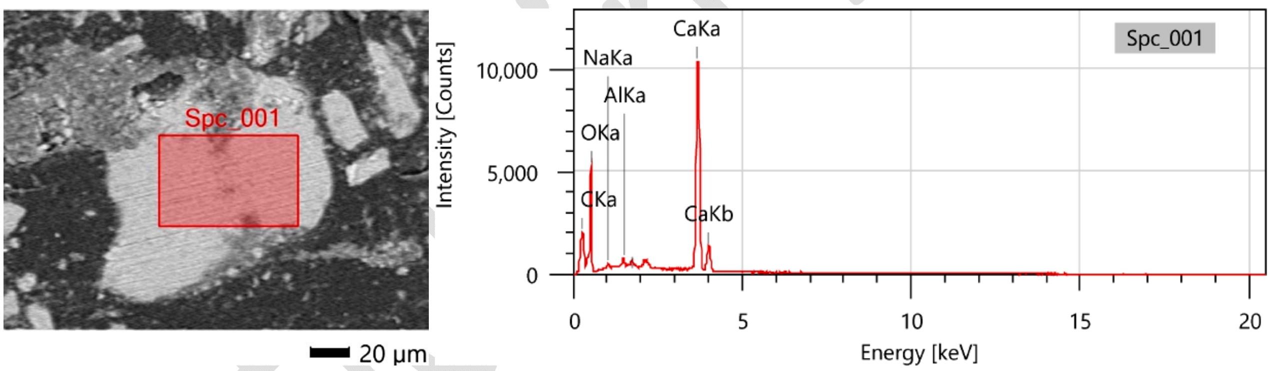

Figure 6. EDS analysis of AGSP with particle size of 180 μm

Importantly, the density changes noticed across different reinforcement conditions are not statistically significant when compared to the matrix alloy. This finding is particularly valuable because it demonstrates that incorporating AGSP does not substantially compromise the lightweight nature of the Al6061 alloy. The relatively low density of AGSP (1.3 g/cm^3) helps maintain the lightweight characteristics of the composite material. Maintaining low density is crucial for applications where weight reduction is a primary design consideration, such as automotive and aerospace components. Therefore, it can be concluded that AGSP reinforcement offers a sustainable material solution while preserving the essential lightweight characteristics of aluminium alloys, making it suitable for applications requiring low-density materials.

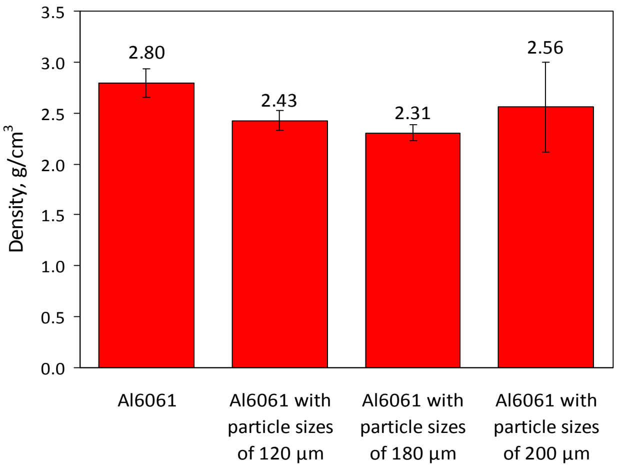

Figure 7. Effect of AGSP particle size on the density of Al6061

3.3 Tensile characteristics

The relationship between stress and strain of each sample is provided in Figure 8 and Table 4. The modulus of elasticity values obtained in this study are relatively low. Previous studies have reported a modulus of elasticity value for Al6061 alloy of 68.9 GPa [27], which is higher than the values measured in the present research. The mould size and cooling rate significantly influence the solidification behaviour and microstructural characteristics of the cast alloy, which in turn affect the mechanical properties, including modulus of elasticity. It has been shown that the size of reinforcement particles plays an important role in determining the tensile properties of aluminium matrix composites. In the present study, relatively coarse particles of 180 and 200 µm produced higher stress concentrations, uneven particle dispersion, and a greater tendency for interfacial debonding between the matrix and reinforcement, leading to a significant decrease in tensile strength [28,29]. In contrast, the finest reinforcement particles (particle sizes of 120 µm) exhibited better dispersion within the matrix and provided a more effective interface surface area, subsequently enhancing interface bonding and a more efficient load transfer process [30].

This is consistent with Owa and Olubambi [31], who reported that poor particle distribution in $CaCO_3$-based shell particle composites led to void formation and reduced tensile strength. In contrast, well-dispersed composites showed superior tensile performance, confirming that dispersion quality, governed here by particle size, is a key factor in biogenic $CaCO_3$-reinforced aluminium MMCs. Furthermore, the tensile properties of the composite with particle sizes of 120 µm did not show significant deviation from the unreinforced alloy, indicating that the addition of AGSP offers a sustainable and useful application for *Anadara granosa* shell waste, which is typically discarded after consumption. Although the tensile strength remains slightly lower than that of the matrix, the reduced density and sustainable use of shell waste justify the incorporation of AGSP as reinforcement.

4. Conclusion

The present study aims to analyse the effect of variations in the particle size of AGSP (120, 180 and 200 µm) on the microstructural characteristics and mechanical properties of Al6061 alloy. The results

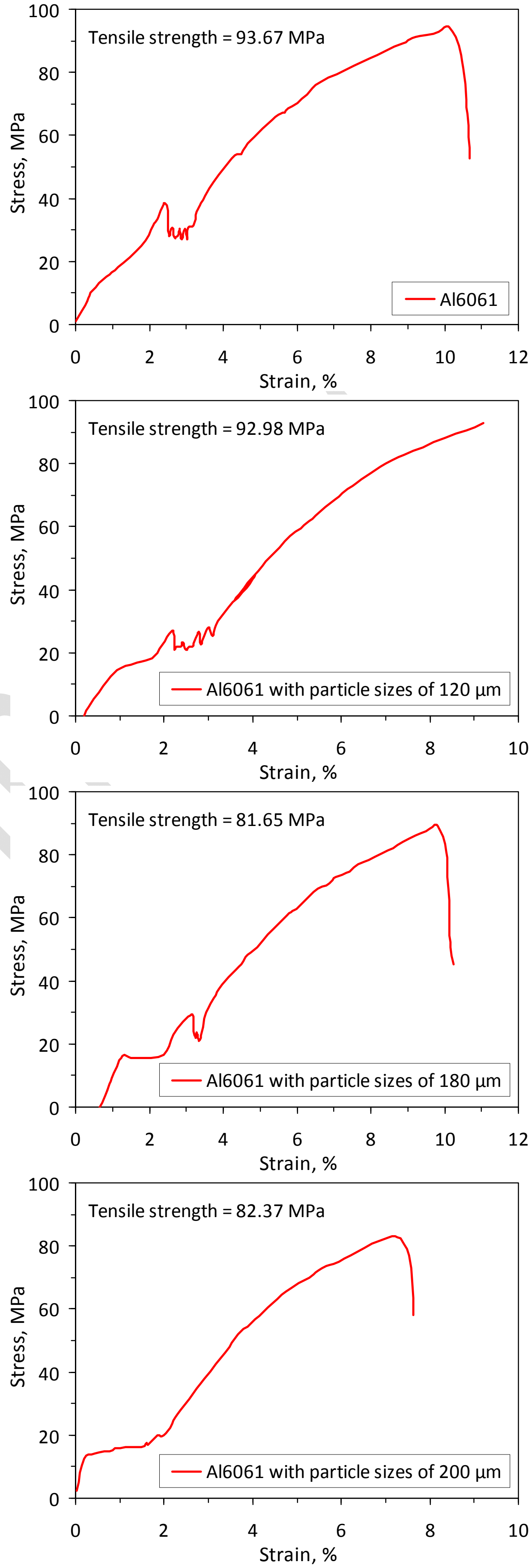

Figure 8. Tensile test results in the form of corresponding stress-strain curves

Table 4. Mechanical properties of the tested samples

Sample	Maximum strain, %	Modulus of elasticity, GPa	Yield strength, MPa	Tensile strength, MPa
Al6061	10.12 ± 0.51	14.27 ± 0.71	38.44 ± 1.92	93.67 ± 4.68
Al6061 with particle sizes of 120 µm	9.20 ± 0.46	12.09 ± 0.60	15.12 ± 0.76	92.98 ± 4.65
Al6061 with particle sizes of 180 µm	6.29 ± 0.31	21.46 ± 1.07	19.77 ± 0.99	81.65 ± 4.08
Al6061 with particle sizes of 200 µm	6.40 ± 0.32	18.30 ± 0.92	23.26 ± 1.16	82.37 ± 4.12

show that particle size plays an important role in particle distribution, structural homogeneity and reinforcement effectiveness in composite materials. The addition of 15 wt. % AGSP slightly reduced the composite density from 2.80 g/cm^3 to 2.31 – 2.56 g/cm^3, preserving the lightweight characteristics of the aluminium matrix. Although the tensile strength of the composites remains slightly lower than that of the unreinforced Al6061 alloy, the reduced density and sustainable use of shell waste justify the incorporation of AGSP as reinforcement.

Variations in particle sizes of 180 and 200 µm resulted in less uniform distribution, while a particle size of 120 µm produced a more homogeneous distribution, thereby improving interfacial bonding quality, reducing potential porosity and contributing to higher tensile performance with tensile strength of 92.98 ± 4.65 MPa, comparable to the unreinforced Al6061 alloy (93.67 ± 4.68 MPa). Finer particles were also found to provide better load transfer efficiency and more stable mechanical properties. Therefore, selecting a particle size of 120 µm is the optimal choice for improving the quality of AGSP-reinforced Al6061 alloy.

References

[1] M. Penchal Reddy, N. Alsaleh, S. Ataya, K. Rama Gopal, A.M.A. Mohamed, Recent advances in fabrication and performance of metal matrix composites (MMCs): A comprehensive review, Journal of Materials Research and Technology, Vol. 39, 2025, pp. 8076-8097, DOI: 10.1016/j.jmrt.2025.11.138

[2] G.B. Veeresh Kumar, C.S.P. Rao, N. Selvaraj, M.S. Bhagyashekar, Studies on Al6061-SiC and Al7075-Al_2O_3 metal matrix composites, Journal of Minerals and Materials Characterization and Engineering, Vol. 9, No. 1, 2010, pp. 43-55, DOI: 10.4236/jmmce.2010.91004

[3] M. Lipińska, F. Pixner, A. Hütter, M. Mras, K. Jaworski, N. Enzinger, M. Lewandowska, Precipitation phenomena in Al_2O_3/Al-Mg-Si metal matrix composites manufactured via friction stir processing, Journal of Alloys and Compounds, Vol. 1036, 2025, Paper 181648, DOI: 10.1016/j.jallcom.2025.181648

[4] Z. Deng, X. Yang, X. Yu, Z. Huang, D. Zhu, M. Shi, High temperature flexural strength, microstructure, phase evolution and anti-oxidation mechanism of Al-coated carbon fiber/boron phenolic resin ceramizable composite modified with TiB_2 and B_4C, Ceramics International, Vol. 49, No. 15, 2023, pp. 25003-25015, DOI: 10.1016/j.ceramint.2023.05.029

[5] S. Salifu, P.A. Olubambi, High entropy alloy reinforced lightweight metal matrix composites: A review of the fundamentals, fabrication, properties, and prospects, Materials Today Sustainability, Vol. 32, 2025, Paper 101216, DOI: 10.1016/j.mtsust.2025.101216

[6] E. Sinurat, F.R. Dewi, D. Fransiska, R. Nurbayasari, Synthesis and characterization of hydroxyapatite of cockle shells (*Anadara granosa*) originated from Indonesia through precipitation method, IOP Conference Series: Earth and Environmental Science, Vol. 1118, 2022, Paper 012035, DOI: 10.1088/1755-1315/1118/1/012035

[7] N.M. Nasir, N. Zainuddin, F.T.V. Wai, Characterization of *Anadara granosa* as a potential source of calcium carbonate for glass ionomer cement formulation, Malaysian Journal of Analytical Sciences, Vol. 27, No. 1, 2023, pp. 8-19.

[8] L.M. Hasan, A.M. Ali, Assessment of eggshell and $CaCO_3$ reinforced recycled aluminium green metal matrix, Journal of Achievements in Materials and Manufacturing Engineering, Vol. 118, No. 2, 2023, pp. 57-61, DOI: 10.5604/01.3001.0053.7662

[9] I.Y. Suleiman, A. Kasim, A.T. Mohammed, M.Z. Sirajo, Evaluation of mechanical, microstructures and wear behaviours of aluminium alloy reinforced with mussel shell powder for automobile applications, Strojniški vestnik – Journal of Mechanical Engineering, Vol. 67, No. 1-2, 2021, pp. 27-35, DOI: 10.5545/sv-jme.2020.6953

[10] M.T. Al Fath, H. Nasution, A. Sinabariba, D. Nugroho, G.C.R. Hasibuan, V. Alexander, M.H.S.

Ginting, R. Sidabutar, N.F. Dalimunthe, M. Syukri, Development of chitosan-based polymer electrolyte membrane from blood clam (*Anadara granosa*) shells with KCl and PVA/PAN blend polymers, Results in Engineering, Vol. 28, 2025, Paper 107465, DOI: 10.1016/j.rineng.2025.107465

[11] W. Saraswati, A. Soetojo, N. Dhaniar, H.A. Praja, R.M. Santoso, N.S. Nosla, G. Cindananti, R.V. Rafli, N. Rahardia, $CaCO_3$ from *Anadara granosa* shell as reparative dentin inducer in odontoblast pulp cells: In-vivo study, Journal of Oral Biology and Craniofacial Research, Vol. 13, No. 2, 2023, pp. 164-168, DOI: 10.1016/j.jobcr.2023.01.003

[12] E. Siswoyo, R.N. Zahra, N.H.A. Mai, A. Nurmiyanto, K. Umemura, T. Boving, Chitosan of blood cockle shell (*Anadara granosa*) as a natural coagulant for removal of total suspended solids (TSS) and turbidity of well-water, Egyptian Journal of Aquatic Research, Vol. 49, No. 3, 2023, pp. 283-289, DOI: 10.1016/j.ejar.2023.04.004

[13] H.N. Ruslan, K. Muthusamy, M.F.M. Jaafar, N.A. Zamri, R.P. Jaya, Mechanical properties of mortar with *Anadara granosa* waste as partial sand replacement, The Open Civil Engineering Journal, Vol. 17, 2023, Paper e187414952303280, DOI: 10.2174/18741495-v17-2305230-2022-85

[14] H. Gassour, M.A.E. Omer, G. Aboelmagd, J. Wang, X. Hao, A. Elsheikh, K. Hamdy, A.M.M. Ibrahim, Green synthesis of silver nanoparticles for enhancing tribological properties of recycled Al6061 matrix composites, Surfaces and Interfaces, Vol. 87, 2026, Paper 109041, DOI: 10.1016/j.surfin.2026.109041

[15] S. Muhammed Muneer, B.S. Arun, V. Renjish, V.N. Aju Kumar, R. Anand Sekhar, Microstructure and mechanical properties of AlNbTaZr-Al_2O_3 refractory high entropy alloy reinforced Al6061 metal matrix composite, Results in Surfaces and Interfaces, Vol. 20, 2025, Paper 100622, DOI: 10.1016/j.rsurfi.2025.100622

[16] P. Beldar, H.R. Kumavat, Comparative analysis of mechanical properties of SiC particle addition on Al6061/Ni and Al6061/Cr metal matrix composites, Materials Letters, Vol. 369, 2024, Paper 136745, DOI: 10.1016/j.matlet.2024.136745

[17] P. Bharathiraja, M. Anthony Xavior, Effect of B_4C and graphene on the microstructural and mechanical properties of Al6061 matrix composites, Journal of Materials Research and Technology, Vol. 31, 2024, pp. 496-505, DOI: 10.1016/j.jmrt.2024.06.098

[18] A. Ghadimyari, F. Akhlaghi, AlFeCuCrNi high-entropy alloy-derived intermetallics and T6 heat treatment: Influence on microstructure and wear of Al6061 matrix composites, Intermetallics, Vol. 189, 2026, Paper 109126, DOI: 10.1016/j.intermet.2025.109126

[19] B.C. Kandpal, J. Kumar, H. Singh, Fabrication and characterisation of Al_2O_3/aluminium alloy 6061 composites fabricated by stir casting, Materials Today: Proceedings, Vol. 4, No. 2A, 2017, pp. 2783-2792, DOI: 10.1016/j.matpr.2017.02.157

[20] ASTM B209-14, Standard Specification for Aluminum and Aluminum-Alloy Sheet and Plate, 2014.

[21] M.Z.A. Khiri, K.A. Matori, N. Zainuddin, C.A.C. Abdullah, Z.N. Alassan, N.F. Baharuddin, M.H.M. Zaid, The usability of ark clam shell (*Anadara granosa*) as calcium precursor to produce hydroxyapatite nanoparticle via wet chemical precipitate method in various sintering temperature, SpringerPlus, Vol. 5, 2016, Paper 1206, DOI: 10.1186/s40064-016-2824-y

[22] Y. Ji, L. Zhang, Q. Dong, X. Song, B. Yang, Microstructure and tensile properties of 6061 aluminum alloy prepared by friction rolling additive manufacturing, Journal of Materials Research and Technology, Vol. 35, 2025, pp. 5464-5474, DOI: 10.1016/j.jmrt.2025.02.197

[23] R.H. Purba, A.N. Septin, J. Julian, E. Armadani, F. Wahyuni, F.M. Mahdhudhu, Influence of *Anadara granosa* shell particle mesh on the microstructure and impact toughness of aluminium 6061 alloy, Applied Engineering Letters, Vol. 11, No. 1, 2026, pp. 44-53, DOI: 10.46793/aeletters.2026.11.1.5

[24] Y. Liao, H. Shi, S. Zhang, B. Da, D. Chen, Particle size effect of oyster shell on mortar: Experimental investigation and modeling, Materials, Vol. 14, No. 22, 2021, Paper 6813, DOI: 10.3390/ma14226813

[25] F.C. Campbell (Ed.), Elements of Metallurgy and Engineering Alloys, ASM International, Materials Park, 2008, DOI: 10.31399/asm.tb.emea.9781627082518

[26] M. Nagaral, K. Raghavendra Pai, V. Auradi, V. Bharath, S. Patil, M.S. Tattimani, Effect of micro graphite particles on the microstructure and mechanical behavior of aluminium 6061 (Al-Mg-Si) alloy composites developed by novel two step casting technique, Journal of Metals, Materials and Minerals, Vol. 31, No. 2, 2021, pp. 38-45, DOI: 10.55713/jmmm.v31i2.1046

[27] Aluminum 6061-T6; 6061-T651, available at: https://asm.matweb.com/search/SpecificMaterial.asp?bassnum=MA6061t6, accessed: 01.06.2026.

[28] R.H. Purba, K. Shimizu, K. Kusumoto, Y. Gaqi, T. Todaka, Effect of boron addition on three-body

abrasive wear characteristics of high chromium based multi-component white cast iron, Materials Chemistry and Physics, Vol. 275, 2022, Paper 125232, DOI: 10.1016/j.matchemphys.2021.125232

[29] M.R. Rezaei, A. Albooyeh, F. Ghafari Golafshani, Effect of matrix particle size on densification behavior, microstructure, and mechanical properties of an Al/FMG/SiC hybrid composite, Silicon, Vol. 15, No. 11, 2023, pp. 4967-4978, DOI: 10.1007/s12633-023-02401-x

[30] Q. Zhao, B. Ju, K. Zhao, J. Zhan, M. Liu, N. Zhang, J. Qian, Z. Xiu, P. Kang, W. Yang, Effect of reinforcement size on mechanical behavior of SiC-nanowires-reinforced 6061Al composites, Materials, Vol. 15, No. 23, 2022, Paper 8484, DOI: 10.3390/ma15238484

[31] A.F. Owa, P.A. Olubambi, Enhancing mechanical properties of aluminium 6063 with crab shell particle reinforcement, Discover Applied Sciences, Vol. 6, No. 7, 2024, Paper 337, DOI: 10.1007/s42452-024-06035-5